ACTA SCIENTIARUM POLONORUM
Acta Sci. Pol. Technol. Aliment. 22(4) 2023, 455–465
www.food.actapol.net pISSN 1644-0730 eISSN 1898-9594 http://dx.doi.org/10.17306/J.AFS.2023.1179

ORIGINAL PAPER

Received: 20.09.2023
Accepted: 06.11.2023

EVALUATION OF THE PHYSICAL AND BIOLOGICAL PROPERTIES OF CHITOSAN FILM COMBINED WITH *CHÚC* (*CITRUS HYSTRIX* DC.) PEEL ESSENTIAL OIL

Do Minh Long[1], Le Pham Tan Quoc[1]✉, Tran Thi Phuong Nhung[1], Tran Thi Huyen[1], Nguyen Le Quynh Nhu[2], Vuong Bao Thy[3]

[1]Institute of Biotechnology and Food Technology, Industrial University of Ho Chi Minh City
12 Nguyen Van Bao Street, Go Vap district, Ho Chi Minh City, 700000, **Vietnam**
[2]Pham Ngoc Thach University of Medicine
2 Duong Quang Trung, district 10, Ho Chi Minh City, 700000, **Vietnam**
[3]Faculty of Health Sciences, University of Cuu Long
National Highway 1A, Phu Quoi, Long Ho, Vinh Long, 85000, **Vietnam**

ABSTRACT

Background. Chitosan (CS) films have gained significant attention and have been extensively utilized in diverse applications, notably in food preservation, owing to their safety and eco-friendliness.
Material and methods. In this study, we evaluated CS films combined with *Chúc* peel essential oil (EO) at concentrations of 0%, 1%, 1.5%, and 2% (v/v). A range of evaluation methods, including Fourier transform infrared (FTIR) spectroscopy, X-Ray diffraction (XRD), and scanning electron microscopy (SEM), as well as assessments of antioxidant activity and physical properties (thickness, opacity, color, permeability, swelling, and solubility), were employed based on their respective application purposes.
Results. The results demonstrated that with increasing EO concentration, the film's thickness, opacity, tensile measurement, and antioxidant activity exhibited a concomitant increase. However, the film's surface presented an increasing degree of unevenness and roughness; in addition, the results also showed that permeability increases steadily with an increase in EO concentration. Such an increase in permeability may not be advantageous for food preservation applications. Interestingly, color variations across the samples were minimal, with all displaying a slight yellow hue, consistent with the film's swelling degree (SD). Spectroscopic analysis further corroborated that no new or different bonds were formed among the various samples. Furthermore, the film's crystallization capability exhibited variations contingent on the EO concentrations.
Conclusion. Adding *Chúc* EO to the CS strongly affects the properties of the film. Depending on usage needs, we can adjust different concentrations of EOs to create films with desired properties.

Keywords: Chitosan films, *Citrus hystrix*, essential oil, food preservation, physical properties

INTRODUCTION

Nowadays, consumers are setting higher standards for food safety and environmental sustainability. As a result, there is an emerging trend in research focusing on food preservation using natural ingredients such as chitosan (CS) and essential oils (EOs) (Rout et al., 2022).

CS, a natural polysaccharide, is derived from the deacetylation of chitin, a process that substitutes the acetyl

✉lephamtanquoc@iuh.edu.vn, phone: 084 906413493, https://orcid.org/0000-0002-2309-5423

group with an amino group (Wrońska et al., 2021). This biopolymer possesses qualities such as biodegradability, biocompatibility, and antimicrobial activity. Intriguingly, these attributes are influenced by the degree of deacetylation and the molecular weight of CS (Honarkar and Barikani, 2009; Younes and Rinaudo, 2015). Thus, CS has many applications in various domains, including in food preservation (Pham et al., 2023), in the removal of oil, fat, and heavy metals in water treatment, and in medicinal contexts as a moisturizer and wound healer (Younes and Rinaudo, 2015; Santos et al., 2020).

Kaffir lime, also known as *Chúc*, whose scientific name is *Citrus hystrix* DC., is a member of the Rutaceae family. This plant thrives in the tropical climates of Southeast Asia (Agouillal et al., 2017). *Chúc* fruit has been used in the beverage industry in Vietnam, while its peel has been discarded. In addition to its culinary significance, *Chúc* peel is a valuable source of EO, which is an abundant byproduct and enhances its economic worth. *Chúc* EO from leaves and peel has a wide range of potential applications: in cosmetics, it serves as a fragrance and aids in reducing dark spots and acne (Lertsatitthanakorn et al., 2006; Lim, 2012). Moreover, *Chúc* EO has been employed as a remedy for digestive ailments, colds, and pain. Its role in food preservation is noteworthy, especially given its demonstrated biological activity, which ranges from insecticidal (mosquito, cockroach, etc.) to antimicrobial (*Pseudomonas aeruginosa*, *Staphylococcus aureus*, *Salmonella typhimurium*, and *Bacillus cereus*) and antioxidant properties ($IC_{50\text{-}DPPH}$ > 250 µg/mL) (Wungsintaweekul et al., 2010; Lim, 2012; Long et al., 2023). Key components of this oil include *β*-pinene, sabinene, limonene, and citronellal. Furthermore, it has been shown to be safe for human use (Agouillal et al., 2017; Lubinska-Szczygeł et al., 2023). Given the outstanding advantages of *Chúc* oil, its application in food technology has great potential.

EOs are frequently combined with CS to enhance the efficacy of food preservation. This approach is evident in studies such as one that combined CS with orange peel EO (Alparslan and Baygar, 2017) and another that combined it with propolis extract (Çoban, 2021). These combinations produce a material layer that boasts increased antibacterial and antioxidant activity and is both easily degradable and environmentally friendly. However, the combination of CS with *Chúc* peel EO has not yet been studied. This combination will undoubtedly change the film's physical, chemical, and biological properties, but the obtained film's quality needs to be carefully evaluated. Exploring this combination could reveal numerous benefits, potentially unearthing novel properties of the film and its application prospects. This is primarily due to the robust biological activity of *Chúc* peel EO and CS's inherent ability to establish chemical bonds.

MATERIALS AND METHODS

Materials

Chitosan (CS) was provided by Nha Trang University. Its characteristics include 90% deacetylation, a white color, and a scale-like appearance. Essential oil (EO) was extracted from the fruit peel of *Chúc*, which originated in Tinh Bien District, An Giang Province, Vietnam (10°37'55.6" N, 104°59'34.8" E), using steam distillation. The fruits were washed and dried naturally at room temperature, then peeled and cut into small pieces. On average, the per-batch yield was 50–60 kg peel/batch. The distillation time was 3 h at 100°C. The yield of the distillation process was about 2.8% (the acid, ester, and saponification values of EO were 0.561 ±0, 10.66 ±1.405, and 11.22 ±1.405 mg KOH/g EO, respectively, while its refractive index was 1.4699 ±0.0002). The extracted oil was stored in a dark glass bottle at room temperature (28 ±2°C).

Chemicals

Acetic acid with a 1% concentration and 99.6% purity was sourced from Xilong (China), as was glycerol. The Mueller Hinton Agar (MHA) medium was obtained from HiMedia (India), and the 2,2-diphenyl-1-picrylhydrazyl (DPPH) was obtained from Sigma (USA). The other chemicals and solvents used met the requisite standards for analysis and research.

Preparation of CS films with *Chúc* peel EO

The film preparation followed the method described by Sun et al. (2017), albeit with slight adjustments. Initially, 2 g of CS was dissolved in 100 mL of 1% acetic acid and stirred at 50°C for 30 min. Subsequently, 0.5% (0.5 mL) of glycerol was introduced, and the mixture was stirred for an additional 10 min. EO was added at four different ratios (0%, 1%, 1.5%, and 2%,

v/v). After this, 1% (w/v) of Tween 80 (relative to the CS solution) was added and stirred for a further 15 min. The prepared mixture was then poured onto a 14.5 cm × 10.5 cm plastic plate and allowed to dry at temperatures between 50°C and 55°C for 30 h. After drying, the films were carefully removed, and their characteristics were evaluated. For reference, the samples were labeled as CS (control), CS-EO 1, CS-EO 1.5, and CS-EO 2. The obtained films were stored in a sealed plastic container at room temperature (28 ±2°C). The studies were carried out in parallel and repeated three times.

Determination of physical properties of film

Determination of film thickness

The dried film's thickness was assessed using an electronic caliper (Mitutoyo, model 500-182-30, USA), with measurements taken at five distinct, random points on the film (Sun et al., 2017).

Determination of film opacity

The absorbance values were measured at a wavelength of 600 nm using a Genesys 20 spectrophotometer (USA). Based on these values, the opacity was determined using the equation (Sun et al., 2017):

$$O = \frac{A_{600}}{L}$$

where

O is the opacity

A_{600} is the absorbance value at a wavelength of 600 nm

L is the thickness (mm).

Determination of film color

The film's color was measured using the CIELAB color space with a Minolta CR-410 instrument (Japan). For consistent measurements, it is imperative that samples are exposed to identical lighting conditions for the same time duration (Sun et al., 2017). In the CIELAB color system, the values are defined as:

- L^*– lightness or darkness (0 represents black, while 100 indicates white)
- a^*– redness when the value is positive and greenness when negative
- b^*– yellowness when the value is positive and blueness when negative.

Determination of water vapor permeability

The film was cut into a square measuring 6 cm × 6 cm and used to seal the mouth of a 15-mL glass beaker containing distilled water. The beaker was then weighed, its weight was recorded, and it was subsequently placed in a desiccator containing pre-dehydrated silica gel. The desiccator was kept at room temperature (28 ±2°C). After 24 h, the glass beaker was removed from the desiccator and weighed once more. The water vapor permeability of the film was calculated using the following formula (Elshamy et al., 2021):

$$WVTR = \frac{\Delta w}{\Delta t \times S}$$

where

$VWTR$ represents the water vapor transmission rate

Δw is the weight loss of the sample

Δt stands for the storage time (24 h in this case)

S denotes the film's contact area.

Determination of swelling degree (SD)

The process to test film swelling involved submerging a pre-weighed, dry film piece measuring 4 cm × 4 cm in both pure water and a phosphate buffer. This immersion was maintained at room temperature (28 ±2°C) for intervals of 1, 2, and 3 h.

The swelling degree (SD) was then determined using the equation (Santos et al., 2019):

$$SD = \frac{W_s - W_0}{W_0 \times 100\%}$$

where W_0 and W_s represent the weights of the dry film and the film after swelling, respectively. Note: 100% multiplied by the whole expression.

Determination of water solubility

Square samples of the film, each measuring 5 cm × 5 cm, were cut and weighed. These samples were then immersed in 50 mL of water kept at 25°C for 24 h. After this period, the samples were dried until they reached a constant weight at a temperature of 105°C. The weight of the samples after drying was then noted. The water solubility of the film was determined using the following equation (Elshamy et al., 2021):

$$WS\% = \frac{W_{t0} - W_{t24}}{W_{t0} \times 100\%}$$

where

WS represents the water solubility of the film (%)
W_{t0} is the initial weight of the film (g)
W_{t24} is the weight of the film after drying (g)
Note: 100% multiplied by the whole expression.

Determination of tensile measurement

A tensile testing machine, INSTRON model 5543 (USA), was used to measure the tensile strength of the film, which measured 10 cm × 1 cm. The testing was conducted at a speed of 0.1 mm/s until the film broke, all under room-temperature conditions (28 ±2°C). The results were derived from the stress-strain and force-distance curves (Elshamy et al., 2021).

Determination of antioxidant activity

The antioxidant activity was determined using the DPPH radical scavenging assay. The method used was based on that described by López-Mata et al. (2015), with minor modifications. A 1 g portion of the film was weighed and soaked in ethanol (96%) for 2 h. From this solution, 1 mL was extracted and mixed with 2 mL of 0.1 mM DPPH. The resulting mixture was shaken and then incubated in a dark room at room temperature for 30 min. The absorbance was subsequently measured at a wavelength of 517 nm using a UV-Vis spectrophotometer. The antioxidant activity, as determined by the DPPH assay, was calculated using the following equation:

$$\%DPPH = \frac{(A_0 - A_1)}{A_0 \times 100\%}$$

where
A_0 represents the absorbance of the blank solution (DPPH solution)
A_1 indicates the absorbance of the sample solution (DPPH solution and extract)
Note: 100% multiplied by the whole expression.

Fourier transform infrared (FTIR) analysis

Fourier transform infrared (FTIR) analysis was conducted using a Bruker Tensor 27 FTIR spectrometer (Bruker Optik GmbH, Ettlingen, Germany). Spectra were recorded in the range of 4,000 to 400 cm^{-1} with a KBr beam splitter at a resolution of 1 cm^{-1}.

X-Ray diffraction (XRD) analysis

The X-ray diffraction analysis (XRD) was performed on a Bruker AXS D8 ADVANCE ECO X-ray diffractometer (Karlsruhe, Germany). The instrument was supplied with a power of 220 V at 50 Hz and 1 kVA. During the XRD analysis, the operational voltage and current were set to 40 kV and 25 mA, respectively. The analysis involved an angle variation within the 2θ range, and the scanning speed was set at 0.2 rad/s.

Analysis of film structure and morphology with scanning electronic microscopy (SEM)

Scanning electron microscopy (SEM) analysis was performed on a JSM-IT200 scanning electron microscope (JEOL, Japan). The accelerating voltage was set to 5 kV, with magnification ranging between 40 and 10,000 times. After natural drying, samples were coated with platinum using an auto-fine coater (JEC-3000FC, JEOL, Japan).

Data analysis

Three independent measurements were conducted, and the outcomes were presented as the mean ± standard deviation. STATGRAPHICS Centurion XV software was utilized for the statistical assessment of results, applying one-way analysis of variance (ANOVA) and Fisher's least significant difference (LSD) method. A significance level of 5% was adopted.

RESULTS AND DISCUSSION

Physical properties of film

Film thickness

It can be seen from the results in Table 1 that the thickness of the film increases as the concentration of EO increases. Specifically, the thickest film was observed for CS-EO 2, measuring 0.11 mm, while the thinnest was the control sample at 0.063 mm. This result is

Table 1. Film thickness

Type of film	Film thickness, mm
CS	0.063^{a} ±0.006
CS-EO 1	0.086^{b} ±0.006
CS-EO 1.5	0.10^{bc} ±0.01
CS-EO 2	0.11^{c} ±0.01

Different letters (a, b, and c) in the same column indicate statistically significant differences at the 95% confidence level.

consistent with the studies of Filho et al. (2020) and Li et al. (2021), which showed that as it is added in increasing amounts, EO disperses as oil droplets in the film matrix and disrupts intermolecular interactions between CS, breaking its dense network structure and increasing free volumes and the mobility of macromolecules of the films. Generally, the chemical composition of EOs is partly responsible for the thickness of films.

The changes of thickness may affect different film properties, from water vapor permeability, density, and mechanical strength to preservation of the intrinsic qualities of encapsulated substances. Thus, comprehensive evaluations across various factors are essential to discerning the ideal film formulation.

Film opacity

Opacity is a crucial metric for assessing the quality of film products. The materials utilized in film preparation can greatly influence the resultant film quality. Sun et al. (2017) demonstrated this by using CS films combined with polyphenols from thinned young apples (0–1%, w/v), achieving opacities ranging from 0.71 to 4.25 A/mm. In our study, the opacity ranged from 2.294 to 3.057 A/mm. Notably, when EO was incorporated, there was a marked increase in opacity compared to the control sample, as shown in Table 2.

The onset of opacity can be attributed to the migration of EO droplets, which tend to cluster on the film's surface during the drying phase, resulting in surface irregularities. A higher concentration of EO leads to a more pronounced presence of these droplets on the film surface, explaining the observed alterations in opacity (Sánchez-González et al., 2010).

Table 2. Film opacity

Type of film	Film opacity, A_{600}/mm
CS	2.294^{a} ±0.149
CS-EO 1	2.865^{b} ±0.063
CS-EO 1.5	2.943^{b} ±0.089
CS-EO 2	3.057^{b} ±0.170

Different letters (a and b) in the same column indicate statistically significant differences at the 95% confidence level.

Moreover, the studies by Sun et al. (2017) and Elshamy et al. (2021) reported that the opacity values of all their films did not exceed 5. This suggests that the EO concentration used in our study aligns well with the results of these studies. Generally, a film with a lower opacity will be more transparent, making it more suitable for food preservation. This transparency allows customers to easily view the contents of a product wrapped in an edible film.

Film color

Color variations between samples were observed across all three values of L^*, a^*, and b^* ($p < 0.05$). However, the changes seemed erratic, and the differences were almost imperceptible to the naked eye.

Table 3 shows that the combination of EO and CS does not significantly affect the values of a^* and L^*. Conversely, the film exhibits a slight yellowish tint ($b^* > 0$). According to López-Mata et al. (2013), the yellow hue can be attributed to the inherent properties of CS, as this color is related to the presence of the β-(1→4)-2-amino-2-deoxy-D-glucopyranose chain.

Table 3. Film color

Type of film	L^*	a^*	b^*
CS	93.06^{a} ±0.48	-0.96^{a} ±0.04	7.12^{a} ±0.25
CS-EO 1	93.30^{a} ±0.22	-1.15^{c} ±0.03	8.58^{c} ±0.26
CS-EO 1.5	93.35^{ab} ±0.21	-1.06^{b} ±0.03	7.98^{b} ±0.21
CS-EO 2	93.86^{b} ±0.11	-1.06^{b} ±0.04	7.77^{b} ±0.20

Different letters (a, b, and c) in the same column indicate statistically significant differences at the 95% confidence level.

Water vapor permeability

According to Table 4, there was a progressive increase in the water vapor permeability of the films from CS to CS-EO 2. The highest permeability was observed in CS-EO 2 at 795.07 g/m^2/day, while the lowest was in CS at 631.95 g/m^2/day. This heightened permeability with the inclusion of *Chúc* EO in CS films makes them less suitable for food preservation applications. Such findings align with the report of Bonilla et al. (2012), which showed that as the concentration of basil and thyme EOs increases, the water vapor permeability of

Table 4. WVTR of film

Type of film	WVTR (g/m²/d)
CS	631.95^{a} ±17.62
CS-EO 1	642.76^{a} ±18.08
CS-EO 1.5	676.32^{ab} ±7.677
CS-EO 2	795.07^{b} ±128.9

Different letters (a and b) in the same column indicate statistically significant differences at the 95% confidence level.

the film also increases. This phenomenon can be attributed to the excessive amount of oil in the film weakening the intermolecular forces among the polymer chains; the reduction in forces facilitates segmental motion, generating more free space and subsequently enabling water to escape more readily. In contrast, López-Mata et al. (2013) reported that integrating carvacrol EO with CS prepared from shrimp chitin (deacetylation degree of 34%) significantly lowered water vapor permeability compared to the control sample ($p < 0.05$). Interestingly, no difference was found when the carvacrol concentration was increased. The authors revealed that this issue could be related to the presence of microspheres on the surface of the film producing a more compact network, decreasing the WVTR. In addition, Sánchez-González et al. (2010) also found that the water vapor permeability of CS film (deacetylation degree of 82.7%) substantially declined with increasing concentrations of tea tree EO. These observations underscore the influence of both the nature of CS and the chemical composition of the EO on variations in water vapor permeability.

Furthermore, water vapor permeability depends on the chemical structure of the CS film and the prevailing ambient temperature. Ideally, this permeability should be minimal, serving as an indicator of the film's capacity to counter moisture transfer or its efficacy in reducing moisture transfer between food and the environment (Elshamy et al., 2021).

Swelling degree analysis

The SD of the films is presented in Table 5. The samples were immersed in both distilled water and phosphate buffer for varying durations of 1, 2, and 3 h.

The results indicate that films immersed in distilled water exhibit an SD approximately double that of those immersed in phosphate buffer. However, within the same immersion time and solvent, there was no significant difference in SD between the CS samples, regardless of the concentration of added EO. This observation aligns with the findings of Ferreira et al. (2022), who reported that adding andiroba oil to CS did not significantly alter the SD, even with increasing EO concentrations. Contrarily, Santos et al. (2019) discovered that CS films, when combined with clove and tea tree EOs, showed a substantially higher SD in phosphate buffer compared to water. These differences suggest that the SD might be influenced by the binding agents involved, particularly the nature of CS and the type of EO.

Table 5. Swelling degree of film

SD, %		CS	CS-EO 1	CS-EO 1.5	CS-EO 2
After 1h	Water	298.75^{b} ±6.85	253.95^{ab} ±56.3	240.10^{a} ±19.21	239.36^{a} ±13.7
	pH Buffer	157.42^{b} ±16.17	126.48^{ab} ±17.22	93.57^{a} ±21.46	134.76^{b} ±20.99
After 2h	Water	256.34^{a} ±24.92	226.78^{a} ±33.9	249.91^{a} ±43.23	266.47^{a} ±34.9
	pH Buffer	138.16^{b} ±20.99	107.28^{ab} ±19.15	89.51^{a} ±7.14	119.19^{ab} ±33.64
After 3h	Water	298.50^{a} ±12.22	260.39^{a} ±25.13	275.04^{a} ±39.27	294.95^{a} ±10.9
	pH Buffer	149.42^{bc} ±5.61	132.76^{ab} ±15.09	104.60^{a} ±7.91	166.21^{c} ±24.74

Different letters (a, b, and c) in the same row indicate statistically significant differences at the 95% confidence level.

Water solubility

Water solubility plays a pivotal role in determining a film's resistance to water (Sun et al., 2017). As displayed in Table 6, the water solubility percentage of CS films integrated with *Chúc* EO exhibited a decline (from 35.02 to 30.61%). However, the difference was not statistically significant ($p > 0.05$). This result is consistent with the report by López-Mata et al. (2015) that the incorporation of cinnamon oil into CS films led to a decrease in water solubility, which was attributed to the diminished hydrophobicity as a result of the loss of free amino and hydroxyl groups. Controlling the water solubility value during the film preparation process can be an intricate process, given that CS properties might differ based on their source, degree of acetylation, and molecular weight (López-Mata et al., 2015). In addition, the water solubility of the film can be affected by the presence of a plasticizer used in the film-making process (Park et al., 2002). In this case, the obtained results show that the characteristics of CS play a decisive role in water solubility compared to the additional oil volume.

Table 6. Water solubility of film

Type of film	Water solubility, %
CS	$35.02^{a} \pm 0.27$
CS-EO 1	$33.74^{a} \pm 0.88$
CS-EO 1.5	$31.78^{a} \pm 2.49$
CS-EO 2	$30.61^{a} \pm 5.82$

The same letter (a) in the same column indicates no statistically significant differences at the 95% confidence level.

Tensile measurement

As depicted in Table 7, there is a noticeable difference in the tensile measurements of the films ($p < 0.05$) as the concentration of EO changes. The tensile measurement increases with increasing EO concentration, ranging from 1.08 N to 3.06 N. This can be explained by the fact that beyond the inherent biological activity of EO, the tensile measurement might be influenced by the solvent used to dissolve the CS during film preparation, giving it a viscous character. In addition, many other factors can influence the mechanical properties of the film, such as the degree of deacetylation of chitosan and the pH of the solution. Additionally, the EO might act as an effective plasticizer, enhancing the flexibility of the film and reducing its stiffness (Santos et al., 2019).

Table 7. Tensile of film

Type of film	Tensile of film, N
CS	$1.08^{a} \pm 0.02$
CS-EO 1	$1.49^{b} \pm 0.33$
CS-EO 1.5	$1.75^{b} \pm 0.07$
CS-EO 2	$3.06^{c} \pm 0.11$

Different letters (a, b, and c) in the same column indicate statistically significant differences at the 95% confidence level.

In our study, we found that the addition of *Chúc* EO to the CS films positively impacted their tensile measurement. Our results are similar to those of Santos et al. (2019), who reported that adding clove or tea tree EOs to CS films lessened their stiffness and increased their tensile measurement, which makes them well-suited for bandage applications. Conversely, research conducted by Ojagh et al. (2010) found that introducing a cinnamon EO concentration to the films did not lead to a noticeable enhancement in tensile measurements. Ultimately, the results of our study underscore the importance of customizing the concentration of *Chúc* EO to produce films with desired tensile properties tailored to users' specific needs.

Antioxidant activity of film

The antioxidant activity of the film is an essential property for evaluating its quality. As illustrated in Table 8, the antioxidant activity of the film increases with

Table 8. Antioxidant activity of film

Type of film	Antioxidant activity, %
CS	$44.73^{a} \pm 2.72$
CS-EO 1	$51.18^{b} \pm 0.75$
CS-EO 1.5	$59.69^{c} \pm 0.20$
CS-EO 2	$61.77^{c} \pm 0.68$

Different letters (a, b, and c) in the same column indicate statistically significant differences at the 95% confidence level.

increasing EO concentration, ranging from 44.73% to 61.77%. In particular, the antioxidant activity of CS-EO 2 was the highest at 61.77%, which is 1.5 times greater than the control sample at 44.73%. This finding aligns with the study of López-Mata et al. (2015), which demonstrated a significant increase in the film's antioxidant activity as the EO concentration increased from 0.25% to 1.0%. In addition, another study by López-Mata et al. (2013) reported that the antioxidant effect of CS was significantly enhanced with the addition of carvacrol.

Clearly, there is a strong correlation between the combination of CS and varying EO concentrations and the ability to scavenge DPPH radicals. Films with elevated antioxidant activity offer advantages in food processing and preservation.

Structure and morphology of film surfaces

Figure 1 presents the SEM images depicting the surface morphology of CS and CS-EO films at a magnification of ×10,000. The CS film has a smooth, homogeneous surface with a dense structure. The surfaces of CS-EO 1 and CS-EO 1.5, while still relatively smooth, exhibit some agglomerates, signifying potential mechanical vulnerabilities attributed to the immiscibility of the mixture's components (Santos et al., 2019). Furthermore, the voids observable on the film's surface might originate from the aggregation of EO droplets during the drying process (López-Mata et al., 2015).

The surface of CS-EO 2 appears to be rough and uneven, with voids of various shapes. This may be due to the formation of EO droplets of different diameters that are inhomogeneously distributed within the CS

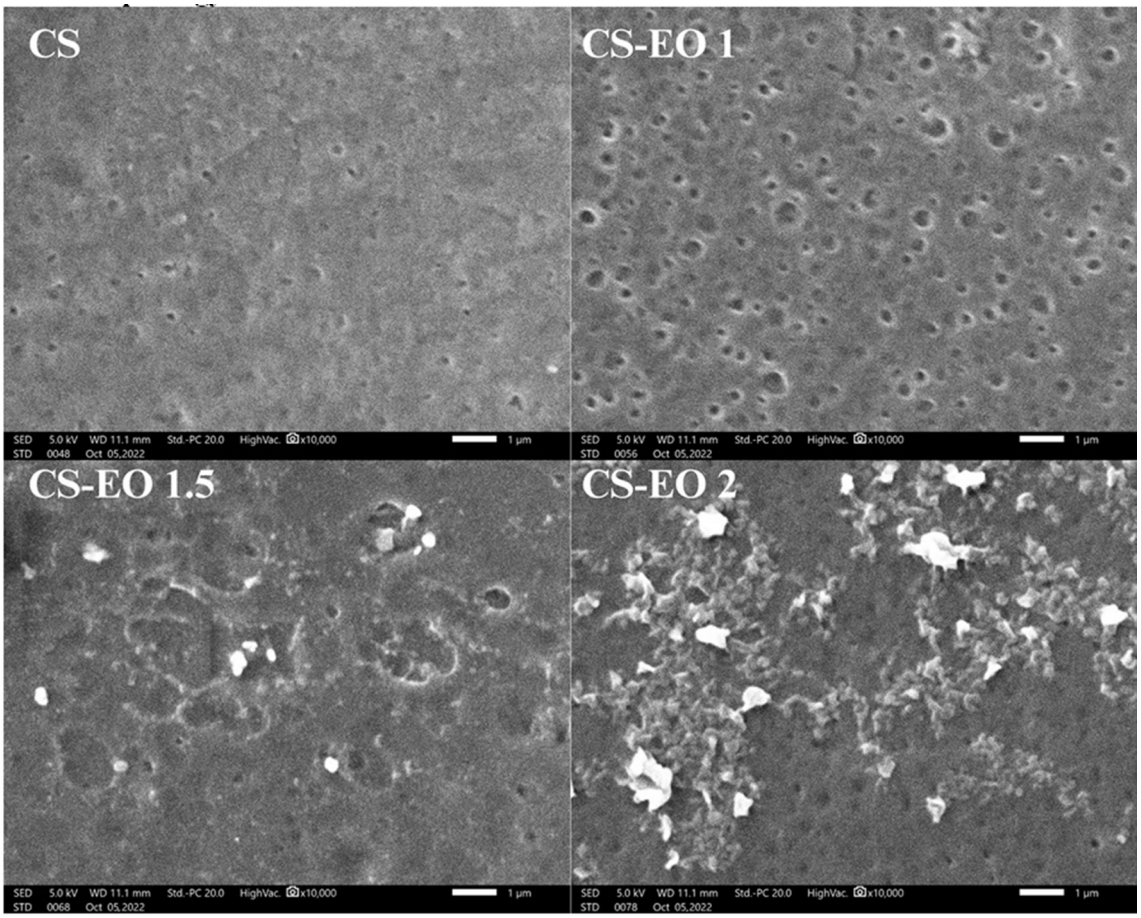

Fig. 1. SEM Images of the films

film. This characteristic depends on the nature of the CS, such as the degree of acetylation and molecular weight (López-Mata et al., 2015). In general, an increase in EO contributes to an increase in aggregation during the drying process. Similar results were also observed by Sánchez-González et al. (2010) when tea tree EO was added to hydroxypropyl methylcellulose film.

Fourier transform infrared spectroscopy (FTIR) analysis

FTIR analysis is one of the preliminary evaluations performed to identify the functional groups of a sample. In our study, the FTIR spectra of CS-EO films are shown in Figure 2. No significant changes were observed in the FTIR spectra of all samples, with all functional groups appearing uniformly.

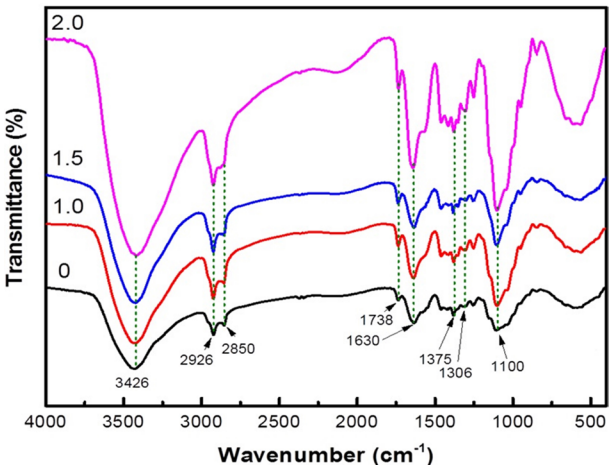

Fig. 2. FTIR analysis of the films

Characteristic peaks shared by all samples were observed in the range of 3,426 to 2,926 cm^{-1}, corresponding to the stretching vibrations of the –OH and –NH groups. The peak at 2,850 cm^{-1} correlates with the stretching vibrations of the C–H group. Additionally, the FTIR spectrum reveals specific absorption peaks at 1,738 cm^{-1}, attributed to the C=O group, and a peak at 1,630 cm^{-1}, associated with the bond of the amide and NH_3^+ groups. The peak at 1,375 cm^{-1} indicates the presence of the phenol group, while the peak at 1,306 cm^{-1} pertains to the S=O group. The peak at 1,100 cm^{-1} is related to the C–O group. These results are similar to the FTIR spectra of CS films documented by Nasef et al. (2011) and Chang et al. (2019).

Based on the results obtained, it is evident that certain compounds in the EOs interact with CS. Specifically, compared to the control sample, interactions between the EOs and the CS lead to alterations in the band intensities.

X-Ray diffraction (XRD) analysis

Figure 3 displays the XRD results for film samples at varying concentrations. The degree of crystallization of CS films is characterized by peaks at angles 2θ = 9–10° and 2θ = 19–20°. When EO is added, the interaction between the EO and the film modifies the crystallization degree, leading to alterations in the peaks and the emergence of new ones. For instance, CS samples with incorporated EOs, namely CS-EO 1, CS-EO 1.5, and CS-EO 2, show a new peak at angle 2θ = 29–30° and a decrease in intensity at angles 2θ = 9–10° and 2θ = 19–20°. A new peak emerges at angle 2θ = 40–41°.

Similarly, a study by Yoncheva et al. (2021) on the microencapsulation of oregano EO using a mixture of CS and alginate showed that a diffraction peak with pronounced intensity at angle 2θ = 20° and a wider peak at angle 2θ = 42° emerged compared to the control sample. This indicates that when EO is added to CS samples, it alters the properties of the film, leading to the formation of new diffraction angles and affecting its crystallization capacity. The specific direction

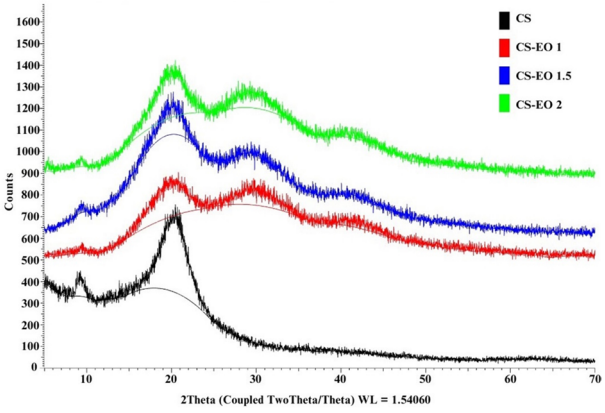

Fig. 3. XRD analysis of the films

of these diffraction peak changes is influenced by the chemical composition of the EO.

CONCLUSION

In conclusion, this study shows that the combination of CS with *Chúc* peel EO significantly alters the properties of the film. These modifications manifest as a slightly yellow hue and diminished transparency, although there is a decrease in the SD. Additionally, the water solubility of the film is reduced, and the 2% EO-supplemented sample displays antioxidant activity that is 1.5 times greater than the control sample. A notable drawback, however, is the increased water vapor permeability, which might be detrimental to food preservation. On the other hand, the addition of *Chúc* peel EO enhances the mechanical properties of the film, specifically its tensile measurement, making the film more adaptable and suitable for food packaging. Moreover, using CS combined with *Chúc* peel EO offers the flexibility to modify the concentration of the EO based on specific application requirements to yield an optimal film. Therefore, CS and *Chúc* peel EO are suitable for application in edible packaging technology to preserve some solid foods with low water activity and moisture, such as cake and candy.

ACKNOWLEDGMENTS

This research was performed at the Institute of Biotechnology and Food Technology, Industrial University of Ho Chi Minh City (Vietnam). The authors would like to thank Doan Thi Thuy Diem and Tran Thi Dieu Thien for their helpful advice on various technical issues examined in this paper.

REFERENCES

Agouillal, F., Taher, Z. M., Moghrani, H., Nasrallah, N., Enshasy, H. E. (2017). A review of genetic taxonomy, biomolecules chemistry and bioactivities of *Citrus hystrix* DC. Biosci. Biotechnol. Res. Asia, 14, 285–305. http://doi.org/10.13005/bbra/2446

Alparslan, Y., Baygar, T. (2017). Effect of chitosan film coating combined with orange peel essential oil on the shelf life of deepwater pink shrimp. Food Bioprocess. Technol., 10, 842–853. https://doi.org/10.1007/s11947-017-1862-y

Bonilla, J., Atarés, L., Vargas, M., Chiralt, A. (2012). Effect of essential oils and homogenization conditions on properties of chitosan-based films. Food Hydrocoll., 26, 9–16. https://doi.org/10.1016/j.foodhyd.2011.03.015

Chang, W., Liu, F., Sharif, H. R., Huang, Z., Goff, H. D., Zhong, F. (2019). Preparation of chitosan films by neutralization for improving their preservation effects on chilled meat. Food Hydrocoll., 90, 50–61. https://doi.org/10.1016/j.foodhyd.2018.09.026

Çoban, M. Z. (2021). Effectiveness of chitosan/propolis extract emulsion coating on refrigerated storage quality of crayfish meat (*Astacus leptodactylus*). CyTA – J Food, 19, 212–219. https://doi.org/10.1080/19476337.2021.1882580

Elshamy, S., Khadizatul, K., Uemura, K., Nakajima, M., Neves, M.A. (2021). Chitosan-based film incorporated with essential oil nanoemulsion foreseeing enhanced antimicrobial effect. J. Food Sci. Technol., 58, 3314–3327. https://doi.org/10.1007/s13197-020-04888-3

Ferreira, E. d. S., Paranhos, S. B., Paz, S. P. A. da, Canelas, C. A. d. A., Nascimento, L. A. S. d., …, Candido, V. S. (2022). Synthesis and characterization of natural polymeric membranes composed of chitosan, green banana peel extract and andiroba oil. Polymers, 14, 1105. https://doi.org/10.3390/polym14061105

Filho, J. G. D. O., Deus, I. P. B. D., Valadares, A. C. F., Fernandes, C. C., Estevam, E. B. B., Egea, M. B. (2020). Chitosan film with *Citrus limonia* essential oil: Physical and morphological properties and antibacterial activity. Colloids Interfaces, 4, 18. https://doi.org/10.3390/colloids4020018

Honarkar, H., Barikani, M. (2009). Applications of biopolymers I: chitosan, Monatsh. Chem., 140, 1403–1420. https://doi.org/10.1007/s00706-009-0197-4

Lertsatitthanakorn, P., Taweechaisupapong, S., Aromdee, C., Khunkitti, W. (2006). In vitro bioactivities of essential oils used for acne control. Int. J. Aromather., 16, 43–49. https://doi.org/10.1016/j.ijat.2006.01.006

Li, Y., Tang, C., He, Q. (2021). ffect of orange (*Citrus sinensis* L.) peel essential oil on characteristics of blend films based on chitosan and fish skin gelatin. Food Biosci., 41, 100927. https://doi.org/10.1016/j.fbio.2021.100927

Lim, T. K. (2012). *Citrus hystrix*. In: T.K. Lim (Ed.), Edible Medicinal and Non-Medicinal Plants. Vol. 4. Fruits (pp. 634–643). Dordrecht: Springer.

Long, D. M., Quoc, L. P. T., Nhung, T. T. P., Thy, V. B., Nhu, N. L. Q. (2023). Chemical profiles and biological activities of essential oil of *Citrus hystrix* DC. peels. Korean J. Food Preserv., 30(3), 395–404. https://doi.org/10.11002/kjfp.2023.30.3.395

López-Mata, M. A., Ruiz-Cruz, S., Silva-Beltrán, N. P., Ornelas-Paz, J. J., Ocaño-Higuera, V. M., …, Shirai, K. (2015). Physicochemical and antioxidant properties of chitosan films incorporated with cinnamon oil. Int. J. Polym. Sci., 2015, 974506. https://doi.org/10.1155/2015/974506

López-Mata, M. A., Ruiz-Cruz, S., Silva-Beltrán, N. P., Ornelas-Paz, J., Zamudio-Flores, P. B., Burruel-Ibarra, S. E. (2013). Physicochemical, antimicrobial and antioxidant properties of chitosan films incorporated with carvacrol. Molecules, 18, 13735–13753. https://doi.org/10.3390/molecules181113735

Lubinska-Szczygeł, M., Kuczyńska-Łażewska, A., Rutkowska, M., Polkowska, Ż., Katrich, E., Gorinstein, S. (2023). Determination of the major by-products of *Citrus hystrix* peel and their characteristics in the context of utilization in the industry. Molecules, 28, 2596. https://doi.org/10.3390/molecules28062596

Nasef, M. M., El-Hefian, E. A., Saalah, S., Yahaya, A. H. (2011). Preparation and properties of non-crosslinked and ionically crosslinked chitosan/agar blended hydrogel films. J. Chem., 8, 513204. https://doi.org/10.1155/2011/513204

Ojagh, S. M., Rezaei, M., Razavi, S. H., Hosseini, S. M. H. (2010). Effect of chitosan coatings enriched with cinnamon oil on the quality of refrigerated rainbow trout. Food Chem., 120, 193–198. https://doi.org/10.1016/j.foodchem.2009.10.006

Park, S. Y., Marsh, K. S., Rhim, J. W. (2002). Characteristics of different molecular weight chitosan films affected by the type of organic solvents. J. Food Sci., 67, 194–197. https://doi.org/10.1111/j.1365-2621.2002.tb11382.x

Pham, T. T., Nguyen, L. L. P., Dam, M. S., Baranyai, L. (2023). Application of edible coating in extension of fruit shelf life: Review. AgriEngineering, 5, 520–536. https://doi.org/10.3390/agriengineering5010034

Rout, S., Tambe, S., Deshmukh, R. K., Mali, S., Cruz, J., …, Oliveira, M.S. (2022). Recent trends in the application of essential oils: The next generation of food preservation and food packaging. Trends Food Sci. Technol., 129, 421–439. https://doi.org/10.1016/j.tifs.2022.10.012

Sánchez-González, L., González-Martínez, C., Chiralt, A., Cháfer, M. (2010). Physical and antimicrobial properties of chitosan–tea tree essential oil. J. Food Eng., 98, 443–452. https://doi.org/10.1016/j.jfoodeng.2010.01.026

Santos, E. P., Nicácio, P. H. M, Barbosa, F. C., Silva, H. N., Andrade, A. L. S., …, Leite, I. F. L. (2019). Chitosan/essential oils formulations for potential use as wound dressing: physical and antimicrobial properties. Materials, 12, 2223. https://doi.org/10.3390/ma12142223

Santos, V. P., Marques, N. S. S., Maia, P. C. S. V., Lima, M. A. B., Franco, L. O., Campos-Takaki, G. M. (2020). Seafood waste as attractive source of chitin and chitosan production and their applications. Int. J. Mol. Sci., 21, 4290. https://doi.org/10.3390/ijms21124290

Sun, L., Sun, J., Chen, L., Niu, P., Yang, X., Guo, Y. (2017). Preparation and characterization of chitosan film incorporated with thinned young apple polyphenols as an active packaging material. Carbohydr. Polym., 163, 81–91. https://doi.org/10.1016/j.carbpol.2017.01.016

Wrońska, N., Katir, N., Miłowska, K., Hammi, N., Nowak, M., …, Lisowska, K. (2021). Antimicrobial effect of chitosan films on food spoilage bacteria. Int. J. Mol. Sci., 22, 5839. https://doi.org/10.3390/ijms22115839

Wungsintaweekul, J., Sitthithaworn, W., Putalun, W., Pfeifhoffer, H. W., Brantner, A. (2010). Antimicrobial, antioxidant activities and chemical composition of selected Thai spices. Songklanakarin J. Sci. Technol., 32, 589–598.

Yoncheva, K., Benbassat, N., Zaharieva, M.M., Dimitrova, L., Kroumov, A, …, Najdenski, H. M.(2021). Improvement of the antimicrobial activity of oregano oil by encapsulation in chitosan–alginate nanoparticles. Molecules, 26, 7017. https://doi.org/10.3390/molecules26227017

Younes, I., Rinaudo, M. (2015). Chitin and chitosan preparation from marine sources structure, properties and applications. Mar. Drugs, 13, 1133–1174. https://doi.org/10.3390/md13031133